Observations of unusually broadened HF radar spectra from heater-induced artificial plasma irregularities

H. Vickers[1] and T. Robinson[1]

Received 29 March 2010; revised 31 January 2011; accepted 21 February 2011; published 4 May 2011.

[1] Cooperative UK Twin-Located Auroral Sounding System (CUTLASS) HF backscatter targets may be artificially produced using the European Incoherent Scatter (EISCAT) HF ionospheric modification facility at Tromsø, Norway. Plasma irregularities created in this way are known to be highly field aligned and usually give rise to radar echoes possessing spectral widths that are much lower than those seen in natural radar auroral data. In this study we present CUTLASS Finland and Iceland observations of heater-induced irregularities; these irregularities gave rise to enhanced spectral width in the Iceland radar backscatter signal, while the width observed by the Finland radar, pointing almost orthogonal to the Iceland beams, remained low. The observations coincided with a period of disturbed ionospheric conditions when faster-flowing natural irregularities were present, poleward of the heated volume, as well as a flow gradient across the heated volume itself. A latitudinal variation of the Doppler velocity measurements was exhibited in both the Finland and Iceland radar observations. We suggest that this flow inhomogeneity, taken together with the geometry of the observing radar beams, would explain not only the broad spectrum of flow components across the heated volume detected by the Iceland radar but also the asymmetry between the spectral widths measured at Iceland and Finland.

Citation: Vickers, H., and T. Robinson (2011), Observations of unusually broadened HF radar spectra from heater-induced artificial plasma irregularities, *J. Geophys. Res.*, *116*, A05301, doi:10.1029/2010JA015516.

1. Introduction

[2] The generation of field-aligned irregularities (FAI) in the high-latitude ionosphere by means of artificial ionospheric modification often requires low geomagnetic activity in order to establish a strong interaction between the modifying HF wave and the *F* region plasma. Such ideal geophysical conditions are not always present because of the unpredictable nature of the solar-terrestrial environment. The behavior and properties of both naturally occurring and artificially generated irregularities can be diagnosed using HF coherent backscatter radars. The Cooperative UK Twin-Located Auroral Sounding System (CUTLASS) comprises a pair of bistatic HF radars at Hankasalmi, Finland (62.32°N, 26.61°E), and Pykkvibaer, Iceland (63.77°N, −20.54°E), that together form part of the Super Dual Auroral Radar Network (SuperDARN) in the Northern Hemisphere. It has been extensively exploited for the purpose of diagnosing artificial FAI, generated using the European Incoherent Scatter (EISCAT) HF ionospheric modification facility at Tromsø, Norway [*Robinson et al.*, 1997, 1998; *Yeoman et al.*, 1997; *Wright et al.*, 2006]. Artificial HF backscatter is usually distinguished from naturally occurring scatter by its lower spectral width [*Eglitis et al.*, 1998; *Dhillon et al.*, 2002], which demonstrates the slow decorrelation of the radar autocorrelation functions (ACFs) and comparatively high temporal coherence of the scattering structures within the sample volume of artificial scatter.

[3] Modest enhancements in the spectral width of artificial backscatter, when they have occurred, have been attributed to, for example, ULF waves [*Wright et al.*, 2004] or associated with the heated region being in daylight while its conjugate point was in darkness [*Blagoveshchenskaya et al.*, 2007]. *Ponomarenko et al.* [1999] also reported enhancements in the spectral width of artificial backscatter by a factor of 5 when the pump frequency was close to the third and fourth harmonics of the electron gyrofrequency. A number of other studies have also reported and investigated mechanisms for enhancements in the spectral width of natural HF backscatter. These were attributed to various processes, including the ionospheric footprint of magnetospheric particle population boundaries [*Baker et al.*, 1995; *Dudeney et al.*, 1998; *Rodger*, 2000; *André and Dudok de Wit*, 2003] and the impact of intermediate-scale structures on the HF radar wavefront [*Vallières et al.*, 2003, 2004]. For natural backscatter, HF radar spectral widths have, on occasion, been reported as being a good proxy for the open-closed boundary (OCB) [*Moen et al.*, 2000; *Chisham et al.*, 2005], where reduced spectral width is observed equatorward of the OCB, and enhanced spectral widths are seen in regions close to the boundary because of small-scale structuring of the

[1]Radio and Space Plasma Physics Group, University of Leicester, Leicester, UK.

0148-0227/11/2010JA015516

convection electric field. Hence, the spectral width is a significant parameter in identifying a wide variety of geophysical processes that occur both naturally and through artificial means. The interrelationship of geophysical and artificially induced phenomena has been documented by several authors to date [e.g., *Blagoveshchenskaya et al.*, 1998, 2001, 2006; *Yeoman et al.*, 2008; *Kendall et al.*, 2010]; nevertheless, further study in this area is important for improving understanding of the complex solar-terrestrial environment.

[4] Bistatic scatter measurements of HF diagnostic waves made during a previously reported experimental investigation at Tromsø revealed variations in the drift velocity of artificial irregularities across the heated volume [*Blagoveshchenskaya et al.*, 2006]. These variations were interpreted as being due either to two different modes of propagation generating irregularities that were horizontally separated or to a temperature gradient drift instability leading to grouping of irregularities at different altitudes. Both mechanisms give rise to a splitting in the Doppler HF spectrum.

[5] The nature of HF backscatter spectra is governed by the characteristics of the ionospheric irregularities from which the backscattered signal originates. For example, vortices in the ionospheric plasma can give rise to such effects as broadening of the HF Doppler spectrum [*André et al.*, 2000], the occurrence of double-peaked Doppler spectra [*Huber and Sofko*, 2000], and an increase in the decay time of artificial FAI due to additional stability supplied with respect to thermal diffusion processes [*Blagoveshchenskaya et al.*, 2007].

[6] Additional spectral components modify the backscatter ACFs of the main component, such that erroneous values of the Doppler velocity and spectral widths are estimated by standard analytic techniques. A strong correspondence between the spatial occurrence of multicomponent spectra, high spectral widths, and large fit errors has also been shown [*André et al.*, 2002]. *Barthes et al.* [1998] showed that spectra containing ionospheric sources and/or ground scatter can be separated out using the multiple signal classification (MUSIC) statistical numerical technique. Further work in this area involving the preprocessing stage of the ACFs has resulted in significant reductions in the spectral width estimates made by the SuperDARN FITACF software and better agreement with values of diffusion coefficients for those conditions [*Ponomarenko and Waters*, 2006]. This work was, however, based on a small nighttime data set containing a relative minority of multicomponent echoes, indicating that large spectral width does not always correspond to multicomponent spectra. Recently, algorithms have been developed to fit ACFs consisting of ionospheric and ground scatter components to determine the effect of multicomponent spectra on SuperDARN convection velocities derived using standard software [*Ponomarenko et al.*, 2008].

[7] In this paper we examine the spectral characteristics of artificial FAI that were produced during a HF heating experiment on 30 October 2000 using the EISCAT ionospheric modification facility. Both CUTLASS HF radars were operated to make observations of the heater-induced phenomena. The experiment was also performed during an interval when the ionosphere was moderately disturbed, such that large regions of naturally occurring *F* region irregularities were present in the CUTLASS observations as well as wave activity in ground-based magnetometer measurements made at Tromsø. The *K* index measured at the Tromsø Geophysical Observatory during this experiment was 3. We focus on an interval during the experiment, between 1800 and 1830 UT, when the spectral widths observed at Iceland were seen to broaden to values higher than those measured at Finland, where the observing direction lies almost perpendicular to that of the Iceland beam that overlooks the heater site. This asymmetry in the spectral widths' measurements has, to our knowledge, not been previously reported. The remainder of this paper is divided into four sections. Section 2 gives an outline of the heating experiment and a description of the diagnostic instruments, section 3 describes the observations that were made using the CUTLASS radars, and section 4 contains a discussion of the experimental observations in relation to previous work and a possible explanation formulated from the current evidence. We conclude the study by summarizing the most significant findings in section 5.

2. Experimental Procedure

2.1. EISCAT Heater

[8] The artificial heating experiment was conducted using the EISCAT facility in Tromsø (69.6°N, 19.2°E). The heater was transmitting ordinary (O) mode polarization waves at 4.04 MHz on Array 2. The reader is referred to *Rietveld et al.* [1993] for a comprehensive description of the Tromsø heater. The heater effective radiated power (ERP) was approximately 150 MW. The heater beam was pointed vertically (0°S) from 1632 until 1820 UT but was redirected to a field-aligned position (−12°S) for the heater-ON cycle beginning at 1824 UT. The beam remained field aligned until the end of the experiment at 2004 UT. The critical frequency, f_OF_2, measured by the EISCAT dynasonde at Tromsø, was above 4 MHz at 1800 UT and diminished to a little below 4 MHz by 1820 UT, implying that for the majority of the interval the HF pump frequency was greater than or very near to the f_OF_2, so the heating was only marginally overdense.

2.2. CUTLASS Radars

[9] In conjunction with the heating experiment, the CUTLASS Iceland radar at Pykkvibaer operated in the 12.1–12.2 MHz band, making 7 s scans across beams 13, 14, and 15, thus dwelling for approximately 2 s in each of the three beam directions, each beam separated by approximately 3.24°. The operation mode employed thus allowed for high temporal and spatial resolution (15 km), the distance to the first range gate being 1470 km in 1.5-hop propagation mode. The CUTLASS Finland radar at Hankasalmi was operated simultaneously in the 8.9–9.1 MHz band, making 7 s scans across beams 3, 4, 5, 6, and 7, with a dwell time of approximately 1 s in each direction. The distance to the first range gate was 480 km in 0.5-hop propagation mode. Figure 1 illustrates the field of view of the Finland-Iceland radar pair, with the Tromsø heater site marked. The nominal centerlines of Iceland beam 15 and Finland beam 5 are indicated since these lie geometrically closest to the Tromsø heater.

3. CUTLASS Observations

[10] Range-time plots of the standard SuperDARN fit parameters, power, drift velocity, and spectral widths, are

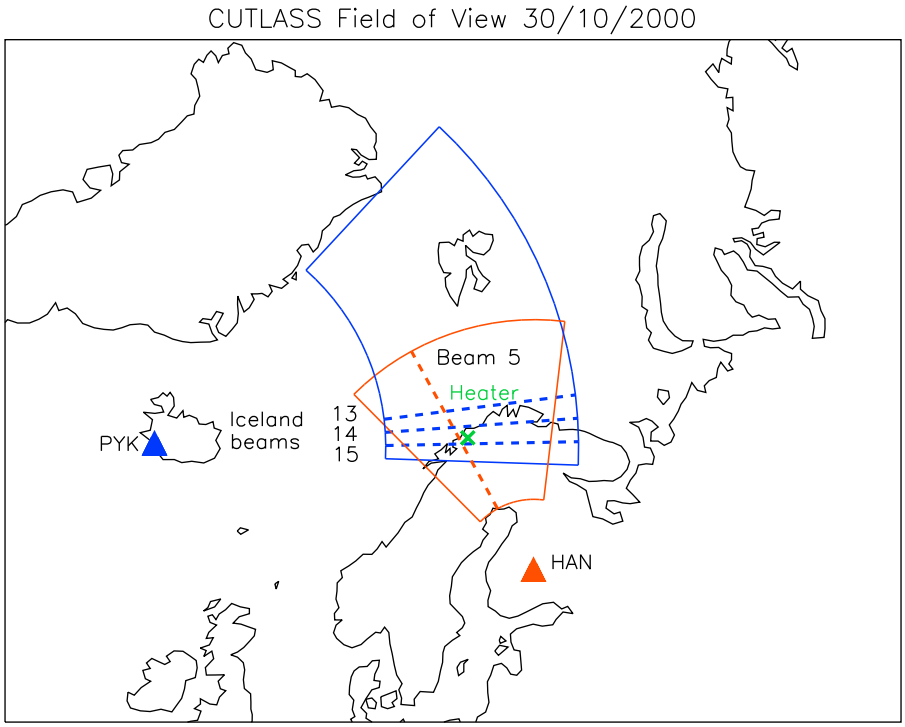

Figure 1. The field of view of the CUTLASS radars in relation to the heating facility in Tromsø, Norway. Locations of the CUTLASS sites in Hankasalmi, Finland, and Pykkvibaer, Iceland, are indicated by the red and blue triangles, respectively; the green X represents the site of the Tromsø heater; and the dashed lines indicate (red) beam 5 of the Finland radar and (blue) beams 13, 14, and 15 of the Iceland radar. The distances to the first range gate from the Finland and Iceland radars are 480 km and 1470 km, respectively.

displayed in Figures 2, 3, and 4, respectively, from 1720 to 1830 UT. Figures 2, 3, and 4 each contain separate plots for the three beams of the CUTLASS Iceland radar (13, 14, and 15) and beam 5 of the CUTLASS Finland radar. The backscatter power measurements for the four radar beams, illustrated in Figure 2, indicate that strong backscatter from artificial FAI in beams 14 and 15 from Iceland, as well as in the Finland beam, was produced throughout the interval until 1830 UT. The artificial scatter can also be seen in Iceland beam 13, albeit at a substantially weaker level in comparison with the other beams. The reason for this is that the artificial irregularities are relatively far from the center of beam 13, where the antenna gain is low (see Figure 1). It must be borne in mind that the scatter power attributed to a given range cell comes from a wide range of beam angles that in the case of the Iceland radar cover several degrees of latitude. An intensification of this weak scatter in Iceland beam 13 is noticeable for the heater-ON period beginning at 1808 UT. As pointed out in section 2.1, the heater frequency was close to the critical frequency throughout; however, the upper hybrid resonance conditions required to produce artificial FAI were clearly met. Other authors have reported observations of artificial FAI under similar marginal conditions [e.g., *Blagoveshchenskaya et al.*, 2006; *Kendall et al.*, 2010]. It is also clear that beams 13 and 14, which are situated northward of beam 15, observed spatially extensive regions of naturally occurring irregularities located closer to the radar than the artificial FAI were (i.e., west of the heated region) and the backscatter power of which was typically 10 decibels higher in beam 13 than in beam 14. It is also evident from the beam 14 and beam 15 observations shown in Figures 2b and 2c that the irregularities drift in a direction toward the Iceland radar as soon as the heater is turned on, as indicated by the change in range with time of the near edge of the artificial backscatter. The effect is particularly noticeable for the four consecutive heater-ON periods beginning at 1800 UT. The rate of change in range is also consistent with the drift velocity of the artificial irregularities, which was of the order of 400 m s^{-1} as measured by the Iceland radar in beam 15, which is shown in Figure 3c. This effect is of interest since it may suggest that the artificial irregularities are being transported out of their source region by the background convection. It is also clear that this drift effect occurs only at the downstream edge of the backscatter patch, as would be expected if the growth time for the artificial irregularities was much shorter than their decay time. The strong artificial backscatter produced in Finland beam 5 also appeared to move in range with time in a direction away from the radar (Figure 2d) but only in the heater-ON period from 1808 to 1812 UT. This motion is consistent with the negative line-of-sight velocities indicating flow away from the radar. The Finland radar also observed regions of natural backscatter at ranges beyond the heated region. This natural scatter was also clearly present at the range gates of the artificial backscatter during the heater-OFF periods when the artificial FAI had disappeared. Hence, it may be deduced

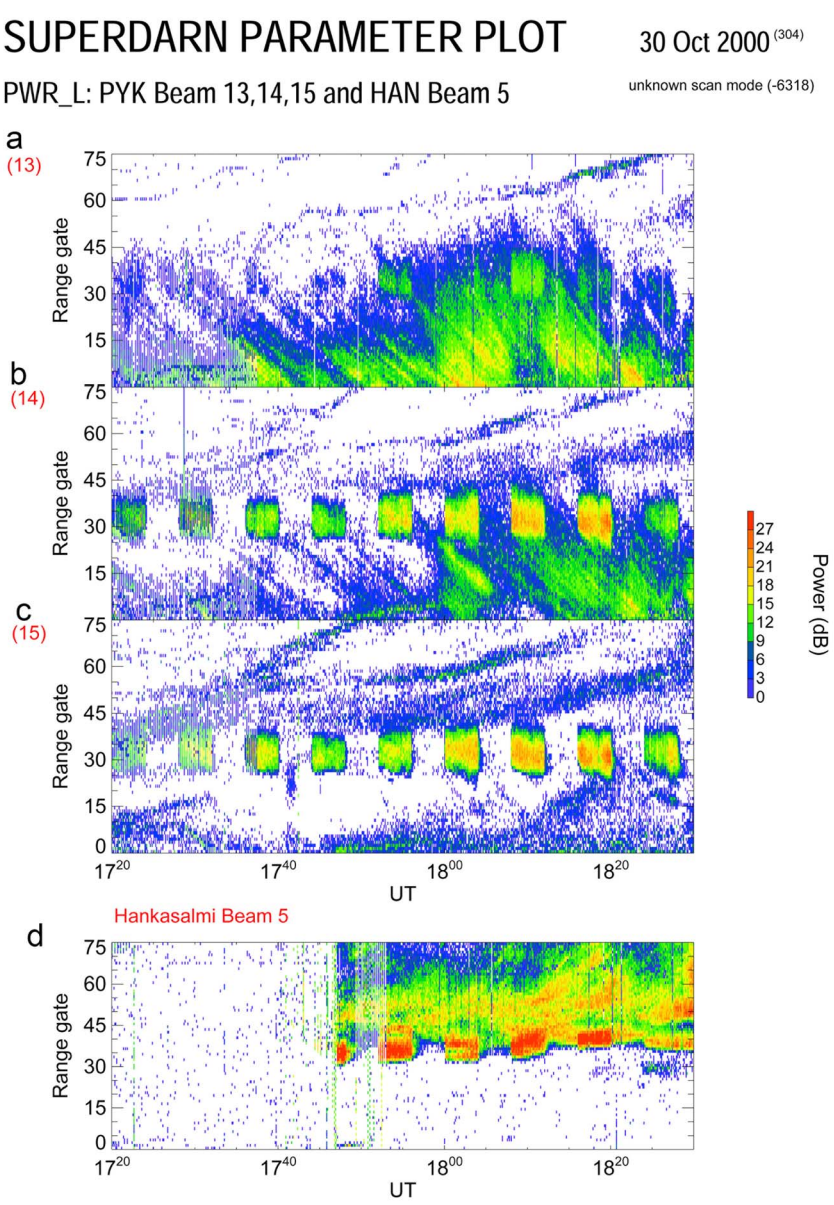

Figure 2. Range-time plots of the SuperDARN FITACF backscatter power detected by the CUTLASS Iceland radar in (a) beam 13, (b) beam 14, and (c) beam 15 and by the CUTLASS Finland radar in (d) beam 5 for artificial heating experiments conducted between 1720 and 1830 UT on 30 October 2000. Note the stronger presence of natural scatter in Iceland beams 13 and 14 as compared with the natural scatter in beam 15, which is centered over the Tromsø heater.

that at range gates 35 to 37 there are underlying natural irregularities with a typical backscatter power of only a few decibels, and these irregularities are colocated with the heated region during both heater-ON periods and heater-OFF periods. We identify natural backscatter as those irregularities that are above the noise threshold of the radar during a heater-OFF period, while artificial backscatter is that which arises from the artificial enhancement of naturally occurring instabilities, previously too weak to be observed by the radar.

[11] The location of the heated region with respect to the CUTLASS beams was also estimated from knowledge of the beam pattern. The artificial FAI backscatter power maximized at range gate 31 or 32 in beam 15, and the beam 15 to beam 14 (maximum) power ratios for each heater-ON period at 1800–1804, 1808–1812, 1816–1820, and 1824–1828 UT were 1.5, 1.09, 1.03, and 2.2, respectively. For the first three of these periods the ratio was reasonably close to unity, which indicated that the heated volume lay roughly halfway between beams 14 and 15. The exception to this was the heater-ON period beginning at 1824 UT, when the direction of the heater beam changed from 0°S to −12°S, and this resulted in a significant increase in the beam 15 to beam 14 power ratio, consistent with a heated region being shifted farther south, closer to the center of beam 15.

[12] Figure 3 shows a striking similarity in the velocities of artificial irregularities detected in the heated patch by all three of the Iceland beams. There are a few incursions of

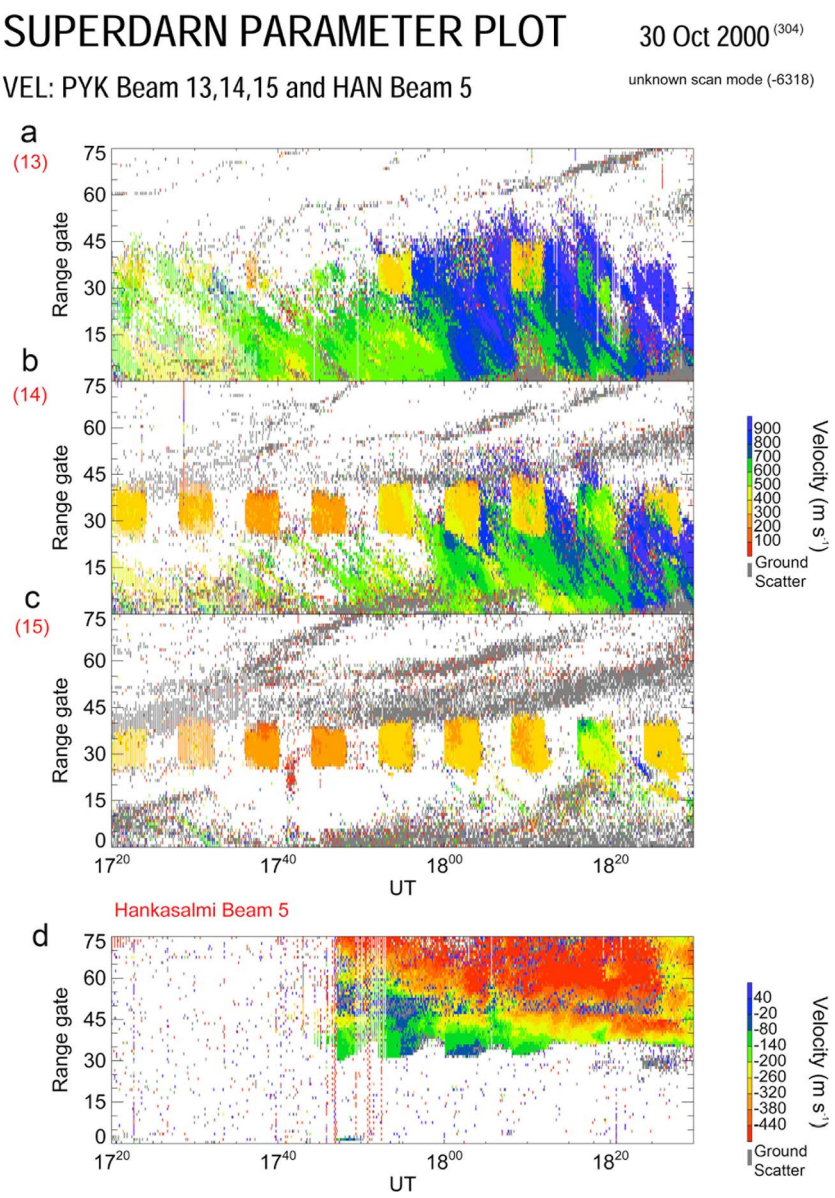

Figure 3. Range-time plots of the SuperDARN FITACF line-of-sight velocity measurements, produced by the CUTLASS Iceland radar in (a–c) beams 13, 14, and 15 and by the CUTLASS Finland radar in (d) beam 5 for the artificial heating experiments conducted between 1720 and 1830 UT on 30 October 2000. Different color scales have been used for the Iceland and Finland observations because of the perpendicular flow directions of the scatter in relation to the radars during this interval. Both ionospheric and ground scatter are shown.

higher-flow scatter populations, probably of natural origin, in beams 13 and 14 during the heater-ON period from 1808 to 1812 UT, but apart from this ON period, the line-of-sight velocities inside the heated patch remain consistently in the ~300 m s^{-1} range throughout the period displayed in Figure 3. It is also apparent that the line-of-sight velocities in the Iceland beams do not change much with range, which indicates little inhomogeneity in the flow in the east-west direction.

[13] The average flow speeds of the natural irregularities present in beams 13 and 14 during a heater-OFF period after 1800 UT were found to be 899 ± 39 m s^{-1} and 682 ± 23 m s^{-1}, respectively, at the center range gates where artificial FAI were produced. These speeds are thus characteristic of the latitudinal convection flow (see Figure 1) at the latitudes at the centers of the respective beams, indicating a significant shear with a slowing toward lower latitudes. There is no significant natural scatter in beam 15, but we can take the Doppler velocity of the artificial scatter as being indicative of the mean flow at this beam's lower latitude [*Hedberg et al.*, 1983; *Hanuise et al.*, 1986; *Eglitis et al.*, 1998]. The mean flow velocity inferred from the artificial FAI during heater-ON periods for beam 15 was 370 ± 70 m s^{-1}. On the basis of this value, the shear appears to extend down

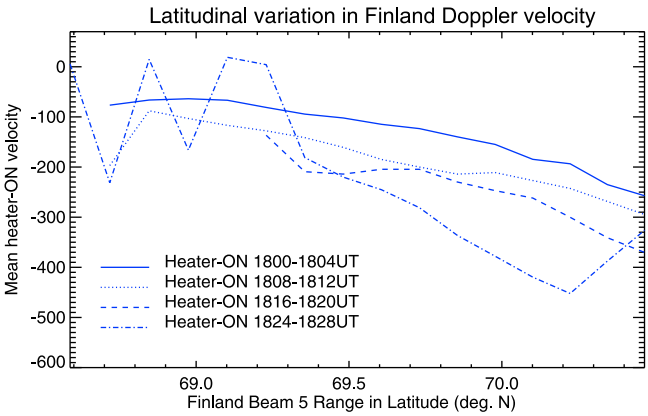

Figure 4. The latitudinal variation in the mean line-of-sight velocity with range along beam 5 measured by the Finland radar. The Doppler velocities were averaged, at each range gate between gates 30 and 45, over an entire heater-ON period for each of the following intervals: 1800–1804, 1808–1812, 1816–1820, and 1824–1828 UT. Since there was a shift with time at the location where the artificial backscatter was produced, the Finland radar did not detect the artificial backscatter at the closer range gates for the later heater-ON periods, and this is indicated by the absence of data points in the lower-latitude limit of the Doppler velocity-range profiles.

to the latitudes of beam 15. The mean Doppler velocities of the largely artificial scatter populations (where these were clearly visible) in beams 14 and 13 were 473 ± 101 m s^{-1} and 570 ± 126 m s^{-1}, respectively. Both of these velocities are significantly lower than the respective mean velocities attributed above to the natural scatter in beams 13 and 14, although they are also somewhat higher than the Doppler velocities of the purely artificial scatter in beam 15. If the scatter in beams 13 and 14 were entirely artificial, then we would expect the Doppler velocities in all three Iceland beams to be very similar since the beam angle to the location of the heated patch would differ by no more than a few degrees, meaning that the three beams would register nearly identical components of the convection flow within the heated patch. The discrepancy could be due to contamination caused by the incursion of natural scatter populations into beams 13 and 14, as was suggested above. However, irrespective of whether the flow speed is obtained from artificial or natural scatter, there are differences among the flow speeds measured by the three Iceland beams, indicative of a latitudinal variation, where the flow speed increases with latitude.

[14] The Doppler velocities measured at Finland with beam 5, also shown in Figure 3, indeed confirm that there is inhomogeneity in the flows across the heated volume (from approximately range gates 30 to 45). Since beam 5 points roughly poleward, this inhomogeneity indicates a north-south gradient in the flow. However, the Finland beam is of course sensitive to the flow component almost orthogonal to that which determines the line-of-sight velocities measured by the Iceland beams. Nevertheless, the tendency for the velocities to increase with increasing latitude is evident in the data from both Finland and Iceland. The flow inhomogeneity inferred from the Finland observations is shown in more detail in Figure 4, where the mean line-of-sight velocities for each heater-ON period are illustrated as a function of range in latitude along beam 5. Because the near edge of the artificial backscatter appears to move to farther ranges from the radar at subsequent heating periods, the lower-latitude limit for each profile is slightly different. However, although the absolute values of the mean Doppler velocities vary between each heating, the gradients in the velocities for each heater-ON flow profile are somewhat similar and correspond to an overall change in the Doppler velocity of about 100 to 150 m s^{-1} over approximately 1.5° in latitude, which is roughly 100 m s^{-1} deg^{-1} in latitude. The exception to this is in the final heating, when the Doppler velocity range is affected by the region of backscatter between approximately range gates 26 to 31, which is detached from the artificial backscatter. This detachment is quite likely responsible for the fluctuations in mean Doppler velocity between 68.6°N and 69.3°N. In contrast, the mean Doppler velocity range profiles observed in Iceland beam 15, shown in Figure 5, exhibit much less variation with respect to range in longitude. Here it is clear that the change in flow speed is of the order of 50 m s^{-1} across a difference of 5° in longitude, or a gradient of 10 m s^{-1} deg^{-1} in longitude. The exception to this, of course, is the 1816–1820 UT heating, when, as noted in Figure 3, short incursions of higher flow were measured in all of the Iceland beams, which therefore resulted in a larger gradient in the mean velocities.

[15] The spectral widths, illustrated in Figure 6 for each radar beam, show that broad backscatter spectra appeared in beam 13 for the whole time interval. Prior to 1800 UT, beam 14 detected backscatter widths that fluctuated between low, typical FAI values and higher values more typical of natural irregularities. The appearance of natural irregularities

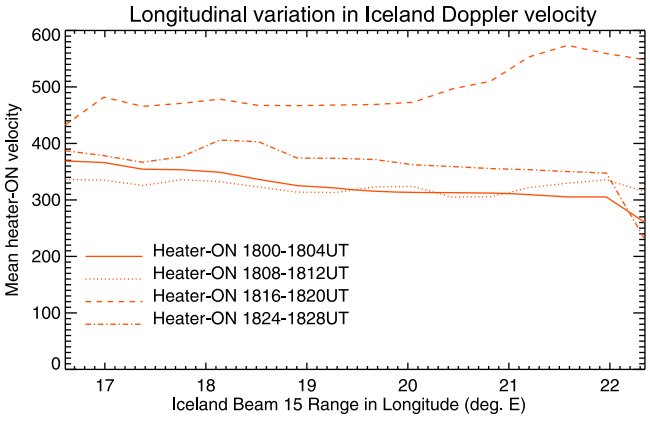

Figure 5. The longitudinal variation in the mean Doppler velocity with range along beam 15 measured by the Iceland radar. The Doppler velocities were averaged, at each range gate between gates 25 and 40 where artificial backscatter was measured, over an entire heater-ON period for each of the following intervals: 1800–1804, 1808–1812, 1816–1820, and 1824–1828 UT. This shows that the flow was relatively homogeneous along the line of sight of beam 15, varying on average by only 10 m s^{-1} deg^{-1} in longitude across the heated patch.

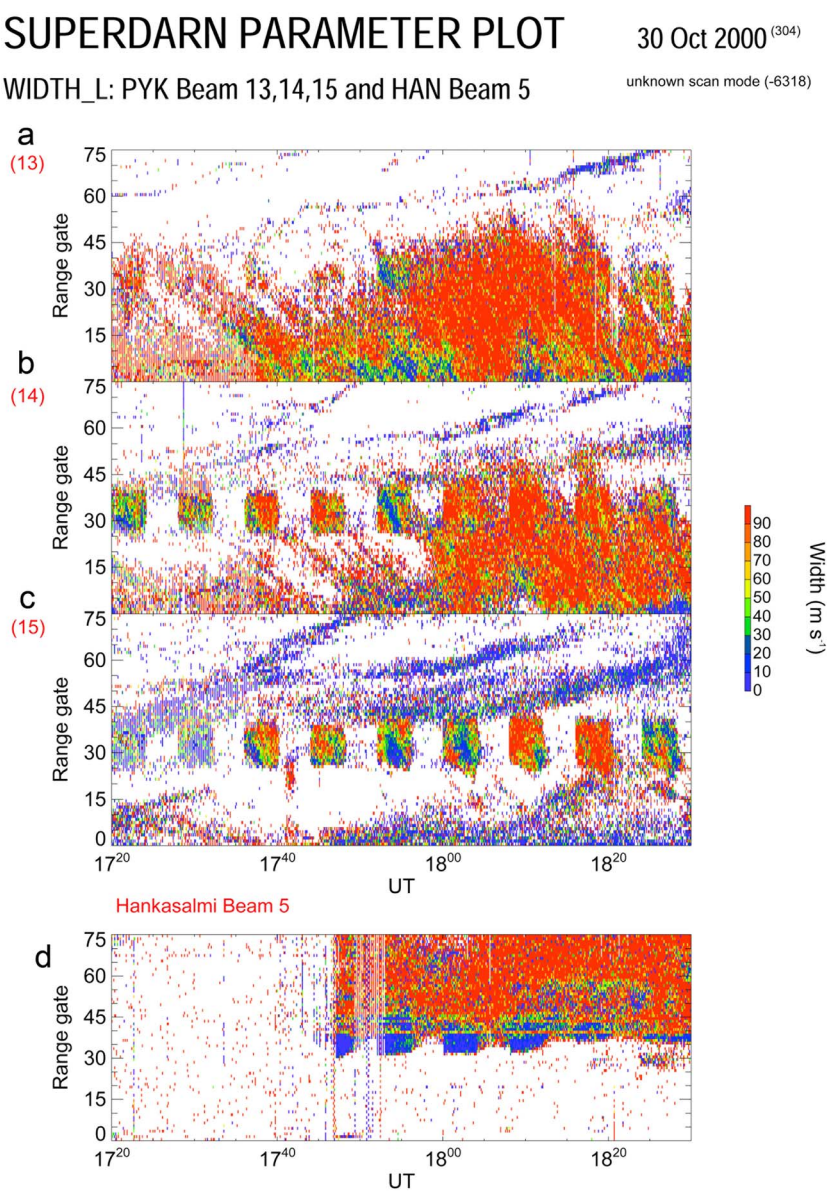

Figure 6. Range-time plots of the SuperDARN FITACF analysis spectral width recorded by the CUTLASS Iceland radar in (a–c) beams 13, 14, and 15 and by the CUTLASS Finland radar (d) beam 5 between 1720 and 1830 UT on 30 October 2000.

at the heater-OFF period beginning at 1756 UT and persisting through the subsequent heater-OFF period thus appears to coincide with an increase in the measured FAI widths in beam 14. The Iceland beam 15 observations showed a noticeable variation in the spectral widths of the artificial backscatter. In particular, there was a transition in the spectral width that occurred at 1800 UT, when relatively high (>100 m s^{-1}) spectral widths were measured during the initial part of the heater-ON period from 1800 to 1804 UT, which in the latter part of the interval diminished to only 10–20 m s^{-1}. These latter widths are more typical values for artificial HF backscatter [*Dhillon et al.*, 2002; *Wright et al.*, 2004]. However, the spectral width during the heater-ON intervals from 1808 to 1812 UT and from 1816 to 1820 UT is in excess of 100 m s^{-1} and remains high across the majority of the range gates where artificial backscatter was produced. This point will be returned to in section 4.

[16] The spectral widths measured by beam 5 of the Finland radar, shown in Figure 6d, are noticeably low at around 10 m s^{-1}, and no broadening of the artificial backscatter appears, even though, as with beams 13 and 14 of the Iceland radar, there is natural backscatter present, which would tend to be associated with higher spectral width. This leads to the unusual condition in which high artificial backscatter spectral width is measured in one direction, while in a direction almost orthogonal to it low width is observed. It is these intriguing observations of the increased spectral widths in Iceland beam 15 in the absence of any obvious natural backscatter and of the asymmetry in the spectral widths measured at Iceland and Finland that are the

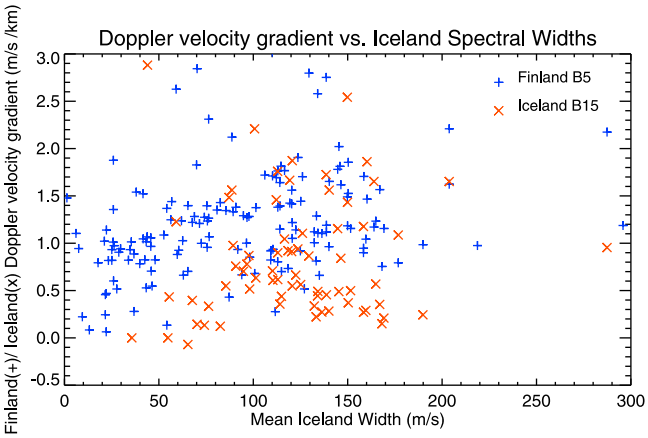

Figure 7. A scatterplot illustrating the relationship between the Doppler velocity gradient within the heated volume and the spectral widths measured by Iceland beam 15. The Doppler velocity gradient measured by the Finland radar (shown by the blue plus signs) was calculated using the observed range extent of artificial scatter and the difference between Doppler velocities at the near and far edges of the artificial backscatter for each heater-ON period. For the Iceland measurements (shown as red Xs), the Doppler velocity gradient was calculated by dividing the difference between the range-averaged line-of-sight velocities measured in beams 13 and 15 by 200 km. This is the approximate spatial separation between the centers of beam 13 and beam 15 at a distance of 2000 km from the Iceland bore site, with beam separation of the order of 6.5°.

focus of the present investigation. In the next section, we discuss these observations in relation to previous studies and offer possible explanations for them.

4. Discussion

[17] This study presents simultaneous CUTLASS observations from Finland and Iceland of artificial HF backscatter produced by the EISCAT heater at Tromsø during an experiment when the ionosphere was disturbed. In contrast to the backscatter typically observed with HF radar under quiet conditions, the artificial backscatter observed in this experiment exhibited unusually high spectral widths of the order of 100 m s^{-1} in one direction (beam 15 at Iceland), while low spectral widths, more typical for heating experiments, of less than 10 m s^{-1} were measured in a direction almost perpendicular to this (beam 5 at Finland). At the same time that the artificial scatter was observed, considerable amounts of natural scatter, flowing at higher speeds, were observed in beams 13 and 14 of the Iceland radar. These beams were centered at higher latitudes than beam 15 and indicated a north-south gradient in the inferred plasma flow speeds. This inhomogeneity was confirmed in the line-of-sight Doppler velocity measurements made by beam 5 of the Finland radar for the heater-ON periods when the spectral broadening was seen in the Iceland radar data.

[18] A number of previous studies of heater-generated irregularities have reported spectral broadening or splitting, and these analyses have tended to offer microplasma or plasma wave processes as an explanation. For example, the effects of the third harmonic of the electron gyrofrequency were considered by *Ponomarenko et al.* [1999], who observed broadening of around 5 Hz. The splitting of up to 2 Hz in Doppler HF spectra from artificial backscatter reported by *Blagoveshchenskaya et al.* [2006] was explained by a drift wave mechanism. In another study the splitting of the HF Doppler spectra from artificial backscatter ranging from 0.5 to 1 Hz was attributed to radial drift of the irregularities and supported by model predictions [*Koloskov et al.*, 2002]. These microplasma processes cannot explain the large spreading reported in section 3. Thus, we must look elsewhere for an explanation.

[19] In our view the result that gives the most telling clue to an explanation of the extreme spectral broadening seen in the Iceland data is the evidence of large latitudinal inhomogeneity in the plasma convection flow, particularly during the two heater-ON periods (1808–1812 and 1816–1820 UT) when the broadening was largest and most persistent. To see the significance of this evidence, one must recall that each data point in the plots in Figures 2, 3, and 6 involves range-beam-time averaging. The time averaging lasts for a few seconds for all the beams and probably does not significantly affect the interpretation of our results. More particularly, the averaging over range is confined to 15 km along the radial direction from the radar location, whereas the averaging over the beam angle, which is typically between 3 and 5 degrees, corresponds to latitudinal distances of around 200 km for the Iceland radar at the range of the heated region and a meridional distance of around 100 km at the (shorter) range of the heated patch from the Finland radar. Consequently, the Finland radar averages over a much shorter distance north-south than east-west and is therefore in contrast to the Iceland radar, which averages over small distances east-west but relatively large distances north-south. Thus, the Iceland radar will average together a relatively broad range of Doppler velocities associated with the flow inhomogeneities that have been noted above, while Finland averages over a relatively homogeneous set of velocities. This effect can be quantified as in Figure 5, which shows that on average, for each heating, the Doppler velocity gradient measured at Iceland beam 15 was only 10 m s^{-1} deg^{-1} in longitude. Since adjacent beams at Finland were separated by roughly 1° in longitude at the range where artificial backscatter was produced, integrating the gradient across this small angular range resulted in a flow difference of 10 m s^{-1}, which is typical of the low artificial backscatter spectral widths measured at Finland.

[20] Figure 7 illustrates further the connection between the latitudinal gradient inferred from the line-of-sight Doppler velocities inside the heated volume and the spectral widths measured at Iceland by beam 15. The Doppler velocity gradient observed at Finland by beam 5 was obtained by taking the difference between the Doppler velocities at the near and far edges of the artificial backscatter and dividing the result by the distance (in km) that separates these range gates. However, in order to obtain the latitudinal velocity gradient indicated by the Iceland measurements, it was necessary to consider the difference between the mean Doppler velocities measured by beam 13 and beam 15. The averaging for the Iceland velocities was performed in the range direction using gates 30 to 40 since this represented the volume common to artificial backscatter observed by

all of the Iceland beams. The difference between the mean Doppler velocities of beam 13 and beam 15 was divided by 200 km, which was taken as a rough estimate of the distance separating the geometric centers of the two beams. A weak positive correlation between the magnitude of the Doppler velocity gradient along the radar line of sight and the spectral widths measured by Iceland beam 15 is exhibited by the gradients inferred from the two radars, despite the fact that they point in almost orthogonal directions. The Doppler velocity gradients measured at both Finland and Iceland fall within the range 0.5–1.5 m s^{-1} km^{-1}. Therefore, an assumption that such a gradient extends into the heated patch would easily explain a spectral broadening of the order of 100 m s^{-1}, a typical measurement at Iceland, over a heated patch around 100 km in width.

5. Summary

[21] We have here analyzed multibeam observations of HF backscatter made with the CUTLASS radars in Finland and Iceland during an ionospheric modification experiment at Tromsø when large regions of natural backscatter were present. Unusual spectral characteristics during the experiment have been identified, where the spectral widths obtained from the SuperDARN FITACF analysis of the Iceland data were broader by at least a factor of 10 compared with widths seen by the Finland radar. Evidence of a north-south shear in the mainly latitudinal plasma convection flows has also been presented, and this, together with considerations of the beam geometry of the radars, has been used to explain the observed broadening and its asymmetry.

[22] **Acknowledgments.** CUTLASS is supported by the Science and Technology Facilities Council (STFC), UK; the Finnish Meteorological Institute, Helsinki; and the Swedish Institute of Space Physics, Uppsala.

[23] Robert Lysak thanks Nataly Blagoveshchenskaya and the other reviewers for their assistance in evaluating this paper.

References

André, R., and T. Dudok de Wit (2003), Identification of the ionospheric footprint of magnetospheric boundaries using SuperDARN coherent HF radars, *Planet. Space Sci.*, *51*, 813–820, doi:10.1016/S0032-0633(03)00115-6.

André, R., M. Pinnock, J.-P. Villain, and C. Hanuise (2000), On the factor conditioning the Doppler spectral width determined from SuperDARN HF radars, *Int. J. Geomagn. Aeron.*, *2*(1), 77–86.

André, R., M. Pinnock, J.-P. Villain, and C. Hanuise (2002), Influence of magnetospheric processes on winter HF radar spectra characteristics, *Ann. Geophys.*, *20*, 1783–1793, doi:10.5194/angeo-20-1783-2002.

Baker, K. B., J. R. Dudeney, R. A. Greenwald, M. Pinnock, P. T. Newell, A. S. Rodger, N. Mattin, and C.-I. Meng (1995), HF radar signatures of the cusp and low-latitude boundary layer, *J. Geophys. Res.*, *100*(A5), 7671–7695, doi:10.1029/94JA01481.

Barthes, L., R. André, J.-C. Cerisier, and J.-P. Villain (1998), Separation of multiple echoes using a high-resolution spectral analysis for SuperDARN HF radars, *Radio Sci.*, *33*(4), 1005–1017, doi:10.1029/98RS00714.

Blagoveshchenskaya, N. F., V. A. Kornienko, A. V. Petlenko, A. Brekke, and M. T. Rietveld (1998), Geophysical phenomena during an ionospheric modification experiment at Tromsø, Norway, *Ann. Geophys.*, *16*, 1212–1225, doi:10.1007/s00585-998-1212-5.

Blagoveshchenskaya, N. F., V. A. Kornienko, T. D. Borisova, B. Thidé, M. J. Kosch, M. T. Rietveld, E. V. Mishin, R. Y. Lukyanova, and O. A. Troshichev (2001), Ionospheric HF pump wave triggering of local auroral activation, *J. Geophys. Res.*, *106*(A12), 29,071–29,089, doi:10.1029/2001JA900002.

Blagoveshchenskaya, N. F., T. D. Borisova, V. A. Kornienko, T. B. Leyser, M. T. Rietveld, and B. Thidé (2006), Artificial field-aligned irregularities in the nightside auroral ionosphere, *Adv. Space Res.*, *38*, 2503–2510, doi:10.1016/j.asr.2004.12.008.

Blagoveshchenskaya, N. F., T. D. Borisova, V. A. Kornienko, V. L. Frolov, M. T. Rietveld, and A. Brekke (2007), Some distinctive features in the behavior of small-scale artificial ionospheric irregularities at mid- and high latitudes, *Radiophys. Quantum Electron.*, *50*(8), 619–632, doi:10.1007/s11141-007-0054-4.

Chisham, G., M. P. Freeman, T. Sotirelis, R. A. Greenwald, M. Lester, and J.-P. Villain (2005), A statistical comparison of SuperDARN spectral width boundaries and DMSP particle precipitation boundaries in the morning sector ionosphere, *Ann. Geophys.*, *23*, 733–743, doi:10.5194/angeo-23-733-2005.

Dhillon, R. S., T. R. Robinson, and D. M. Wright (2002), Radar ACFs and turbulence characteristics from artificially generated field-aligned irregularities, *Geophys. Res. Lett.*, *29*(17), 1830, doi:10.1029/2002GL015364.

Dudeney, J. R., A. S. Rodger, M. P. Freeman, J. Pickett, J. Scudder, G. Sofko, and M. Lester (1998), The nightside ionospheric response to IMF by changes, *Geophys. Res. Lett.*, *25*(14), 2601–2604, doi:10.1029/98GL01413.

Eglitis, P., T. R. Robinson, M. T. Rietveld, D. M. Wright, and G. E. Bond (1998), The phase speed of artificial field-aligned irregularities observed by CUTLASS during HF modification of the auroral ionosphere, *J. Geophys. Res.*, *103*(A2), 2253–2259, doi:10.1029/97JA03233.

Hanuise, C., Å. Hedberg, J. Oksman, E. Nielsen, P. Stubbe, and H. Kopka (1986), Comparison between the ionospheric plasma drift and the motion of artificially induced irregularities as observed by HF backscatter radars, *Ann. Geophys.*, *4*, 49–54.

Hedberg, Å., H. Derblom, B. Thidé, H. Kopka, and P. Stubbe (1983), Observations of HF backscatter associated with the heating experiment at Tromsø, *Radio Sci.*, *18*(6), 840–850, doi:10.1029/RS018i006p00840.

Huber, M., and G. J. Sofko (2000), Small-scale vortices in the high-latitude *F* region, *J. Geophys. Res.*, *105*(A9), 20,885–20,897, doi:10.1029/1999JA000417.

Kendall, E., R. Marshall, R. T. Parris, A. Bhatt, A. Coster, T. Pedersen, P. Bernhardt, and C. Selcher (2010), Decameter structure in heater-induced airglow at the High frequency Active Auroral Research Program facility, *J. Geophys. Res.*, *115*, A08306, doi:10.1029/2009JA015043.

Koloskov, A. V., T. B. Leyser, Y. M. Yampolski, and V. S. Beley (2002), HF pump-induced large scale radial drift of small scale magnetic field-aligned density striations, *J. Geophys. Res.*, *107*(A7), 1097, doi:10.1029/2001JA000154.

Moen, J., H. C. Carlson, S. E. Milan, N. Shumilov, B. Lybekk, P. E. Sandholt, and M. Lester (2000), On the collocation between dayside auroral activity and coherent HF radar backscatter, *Ann. Geophys.*, *18*, 1531–1549, doi:10.1007/s00585-001-1531-2.

Ponomarenko, P. V., and C. L. Waters (2006), Spectral width of SuperDARN echoes: Measurement, use and physical interpretation, *Ann. Geophys.*, *24*, 115–128, doi:10.5194/angeo-24-115-2006.

Ponomarenko, P. V., T. B. Leyser, and B. Thidé (1999), New electron gyroharmonic effects in HF scatter from pump-excited magnetic field-aligned ionospheric irregularities, *J. Geophys. Res.*, *104*(A5), 10,081–10,087, doi:10.1029/1999JA900039.

Ponomarenko, P. V., C. L. Waters, and F. W. Menk (2008), Effects of mixed scatter on SuperDARN convection maps, *Ann. Geophys.*, *26*, 1517–1523, doi:10.5194/angeo-26-1517-2008.

Rietveld, M. T., H. Kohl, H. Kopka, and P. Stubbe (1993), Introduction to ionospheric heating at Tromsø—I. Experimental overview, *J. Atmos. Terr. Phys.*, *55*, 577–599, doi:10.1016/0021-9169(93)90007-L.

Robinson, T. R., A. J. Stocker, G. E. Bond, P. Eglitis, D. M. Wright, and T. B. Jones (1997), O- and X-mode heating effects observed simultaneously with the CUTLASS and EISCAT radars and low power HF diagnostics at Tromsø, *Ann. Geophys.*, *15*, 134–136.

Robinson, T. R., A. Stocker, G. Bond, P. Eglitis, D. Wright, T. B. Jones, and M. T. Rietveld (1998), First CUTLASS-EISCAT heating results, *Adv. Space Res.*, *21*(5), 663–666, doi:10.1016/S0273-1177(97)01000-4.

Rodger, A. S. (2000), Ground-based imaging of magnetospheric boundaries, *Adv. Space Res.*, *25*(7–8), 1461–1470, doi:10.1016/S0273-1177(99)00657-2.

Vallières, X., J.-P. Villain, and R. André (2003), Characterization of frequency effect in SuperDARN spectral width distributions, *Radio Sci.*, *38*(1), 1003, doi:10.1029/2001RS002550.

Vallières, X., J.-P. Villain, C. Hanuise, and R. André (2004), Ionospheric propagation effects on spectral widths measured by SuperDARN HF radars, *Ann. Geophys.*, *22*, 2023–2031, doi:10.5194/angeo-22-2023-2004.

Wright, D. M., T. K. Yeoman, L. J. Baddeley, J. A. Davies, R. S. Dhillon, M. Lester, S. E. Milan, and E. E. Woodfield (2004), High resolution observations of spectral width features associated with ULF wave signatures in artificial HF radar backscatter, *Ann. Geophys.*, *22*, 169–182, doi:10.5194/angeo-22-169-2004.

Wright, D. M., J. A. Davies, T. K. Yeoman, T. R. Robinson, and H. Shergill (2006), Saturation and hysteresis effects in ionospheric modification experiments observed by the CUTLASS and EISCAT radars, *Ann. Geophys.*, *24*, 543–553, doi:10.5194/angeo-24-543-2006.

Yeoman, T. K., D. M. Wright, T. R. Robinson, J. A. Davies, and M. Rietveld (1997), High spatial and temporal resolution observations of an impulse-driven field line resonance in radar backscatter artificially generated with the Tromsø heater, *Ann. Geophys.*, *15*, 634–644, doi:10.1007/s00585-997-0634-9.

Yeoman, T. K., L. J. Baddeley, R. S. Dhillon, T. R. Robinson, and D. M. Wright (2008), Bistatic observations of large and small scale ULF waves in SPEAR-induced HF coherent backscatter, *Ann. Geophys.*, *26*, 2253–2263, doi:10.5194/angeo-26-2253-2008.

T. Robinson and H. Vickers, Radio and Space Plasma Physics Group, University of Leicester, University Road, Leicester, LE1 7RH, UK. (hmsv1@ion.le.ac.uk)